Journal of Coordination Chemistry

ISSN: 0095-8972 (Print) 1029-0389 (Online) Journal homepage: http://www.tandfonline.com/loi/gcoo20

Synthesis, characterization, and antioxidant activity of a new Gd(III) complex

Irena Kostova & Maria Valcheva-Traykova

To cite this article: Irena Kostova & Maria Valcheva-Traykova (2015) Synthesis, characterization, and antioxidant activity of a new Gd(III) complex, Journal of Coordination Chemistry, 68:22, 4082-4101, DOI: 10.1080/00958972.2015.1083557

To link to this article: http://dx.doi.org/10.1080/00958972.2015.1083557

Accepted author version posted online: 27 Aug 2015.
Published online: 11 Sep 2015.

Journal of Coordination Chemistry, 2015
Vol. 68, No. 22, 4082–4101, http://dx.doi.org/10.1080/00958972.2015.1083557

Synthesis, characterization, and antioxidant activity of a new Gd(III) complex

IRENA KOSTOVA*† and MARIA VALCHEVA-TRAYKOVA‡

†Faculty of Pharmacy, Department of Chemistry, Medical University, Sofia, Bulgaria
‡Medical Faculty, Department of Medical Physics and Biophysics, Medical University of Sofia, Sofia, Bulgaria

(*Received 31 May 2015; accepted 24 July 2015*)

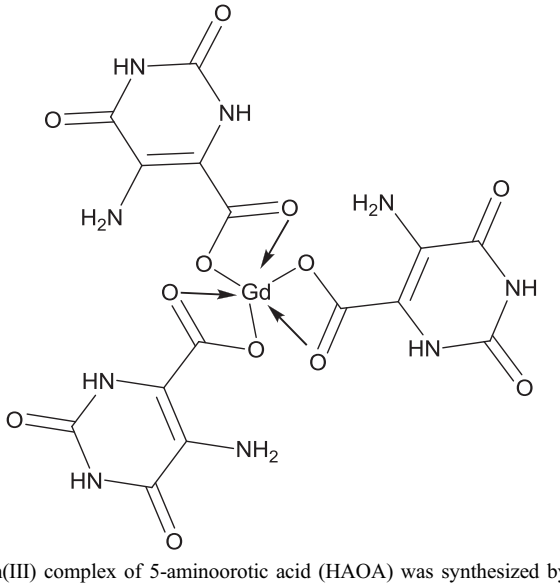

A new gadolinium(III) complex of 5-aminoorotic acid (HAOA) was synthesized by reaction of the respective inorganic salt in molar ratio of 1:3 to ligand. The structure of the complex was determined by elemental analysis, FT-IR, and FT-Raman spectroscopies. Significant differences in the IR and Raman spectra of the complex were observed as compared to the spectra of the free ligand. Detailed vibrational analysis of HAOA and Gd(III)-AOA systems revealed that the binding mode in the complex was bidentate through the carboxylic oxygens. The newly synthesized gadolinium(III) complex of 5-aminoorotic acid (GdAOA) showed antioxidant properties. The antioxidant activity of both HAOA and GdAOA was related with their electron donor properties.

Keywords: Gd(III) complex; 5-Aminoorotic acid; FT-Raman; FT-IR; Antioxidant activity

*Corresponding author. Email: irenakostova@yahoo.com

1. Introduction

Orotic acid (vitamin B_{13}, figure 1) and its salts play an important role in biological systems as precursors of pyrimidine nucleosides and are found in cells and body fluids of many living organisms [1–3]. These compounds are applied in medicine as biostimulators of the ionic exchange processes in organisms, and different metal complexes of orotic acid were studied [4]. There is also a great interest in orotic acid in relation to food protection and nourishment research [5]. Because of the importance of orotic acid and its metal complexes in living systems, a reliable assignment of their vibrational spectra is a useful basis in the study of their interactions with other chemical species present in the biological milieu. The molecular structures of orotic acid and its metal complexes have been determined by Kostova *et al.* [6, 7]. The orotic acid molecule is related to uracil or thymine. Different studies on these types of molecules were done by vibrational spectroscopy [8] as well as normal coordinate analysis and *ab initio* calculations [9, 10]. The results of these studies may help in the assignment of the spectra of orotic acid.

Metal ion complexes of orotic acid (figure 1) and its substituted derivatives continue to attract attention because of its multidentate functionality and pivotal role in bioinorganic chemistry. It is an interesting multidentate ligand capable of coordinating to metal ions through nitrogens, the two carbonyl oxygens, and the carboxylate oxygens [11–16]. Existing studies of its coordination complexes demonstrate that it occurs as a dianion coordinating often via N1 and the carboxylic group, forming a five-membered chelate ring. Despite its polydentate nature, only a few polymeric complexes of orotic acid have been observed.

The multifunctionality of the hydroorotate, $H_2L'^{-}$, and orotate, HL'^{2-}, anions offer interesting possibilities in crystal engineering as a versatile ligand for supramolecular assemblies. Metal ion coordination may occur through the two N atoms of the pyrimidine ring as well as the two carbonyl oxygens or the carboxylic group, which results in a multifaceted coordination chemistry [11–16]. The coordinated orotate anions exhibit a ligand surface with double or triple hydrogen-bonding capabilities, depending on the metal coordination mode, and thus have potential to adopt several modes of interligand hydrogen bonding to allow the formation of extended, self-assembled structures.

Thus, besides the biological relevance, orotic acid and its anions $H_2L'^{-}$, HL'^{2-}, and L'^{3-} are interesting multidentate ligands as they have varied coordination. The equilibrium composition of the reactant mixture and thus the solution pH are critical factors which determine the mode of coordination. The literature lists many reports on the coordinating preferences of the orotate moiety in metal complexes [11–17]. Between pH 3 and 9, orotic acid exists mainly as readily coordinating monodeprotonated $H_2L'^{-}$. Bidentate binding

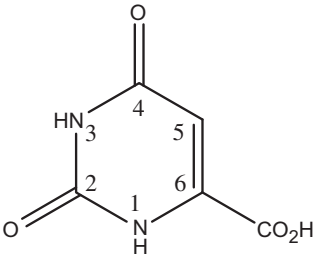

Figure 1. Molecular structure of orotic acid (HOA).

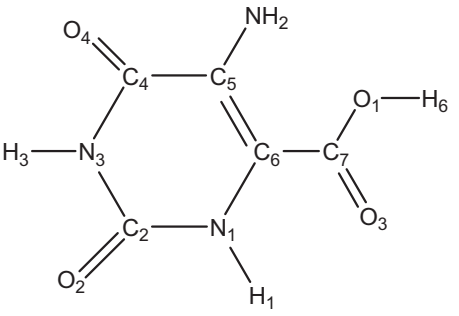

Figure 2. Molecular structure of the 5-aminoorotic acid (HAOA).

through N1 and the carboxylate group was observed by some crystal structure determinations. A recent investigation of nickel(II) complexes of 5-nitroorotate dianion using spectroscopic and theoretical methods revealed novel structural features [17].

Despite the interest in orotate metal complexes, the coordination chemistry of the derivatives of orotic acid has received rather scant attention. One of these derivatives is 5-aminoorotic acid (5-amino-2,6-dioxo-1,2,3,6-tetrahydropyrimidine-4-carboxylic acid, HAOA, figure 2) which has relatively unknown coordination chemistry [18–20]. This ligand has demonstrated versatile coordination modes during the formation of coordination frameworks. Thus, it was a challenge for us to obtain new lanthanide(III) (Ln(III)) coordination complexes with HAOA, especially in view of their application as antioxidant agents. For estimation of the most preferred reactive sites of HAOA for electrophilic attack and metal binding, its geometry was calculated and optimized [18] on the basis of DFT calculations.

Little is known about Ln(III) coordination compounds with HAOA and such Ln(III) complexes, possessing antioxidant and anticancer activity, have not been previously reported. We have recently synthesized lanthanide(III) complexes with a number of biologically active ligands and we have reported their significant cytotoxic activity in different human cell lines [21–25]. These promising results prompted us to search for new lanthanide complexes. Thus, the aim of this work was to synthesize and characterize the complex of gadolinium(III) with HAOA (figure 2) and determine its antioxidant activity. In the present study, we report the synthesis, vibrational (IR and Raman) spectroscopic results, and antioxidant activities of Gd(III) complex of HAOA.

2. Experimental

2.1. *Chemistry*

2.1.1. Reagents. The compounds used for preparing the solutions were Sigma-Aldrich products, p.a. grade: $Gd(NO_3)_3 \cdot 6H_2O$ and 5-aminoorotic acid. HAOA (figure 2) was used as a ligand for the preparation of the metal complex.

2.1.2. Synthesis. The complex was synthesized by reaction of Gd(III) salt and the ligand, in amounts equal to metal:ligand molar ratio of 1 : 3. The synthesis was made in different ratio (1 : 1, 1 : 2, 1 : 3) but in all the cases the final product was with composition 1:3. The

complex was prepared by adding an aqueous solution of Gd(III) salt to an aqueous solution of the ligand, subsequently raising the pH of the mixture gradually to *ca.* 5.0 by adding dilute solution of sodium hydroxide. The reaction mixture was stirred with an electromagnetic stirrer at 25 °C for 1h. At the moment of mixing of the solutions, precipitate was obtained. The precipitate was filtered (pH of the filtrate was 5.0), washed several times with water, and dried in a desiccator to a constant weight. The obtained complex was insoluble in water, methanol, and ethanol, but well soluble in DMSO.

2.1.3. Analytical and spectral methods and instruments. The carbon, hydrogen, and nitrogen contents of the compound were determined by elemental analysis.

The solid-state infrared spectra of the ligand and its Gd(III) complex were recorded in KBr from 4000 to 400 cm^{-1} by an FT-IR 113 V Bruker spectrometer.

The Raman spectra of HAOA and its new Gd(III) complex were recorded with a Dilor microspectrometer (Horiba-Jobin-Yvon, model LabRam) equipped with a 1800 grooves/mm holographic grating. The 514.5-nm line of an argon ion laser (Spectra Physics, model 2016) was used for probe excitation. The spectra were collected in a backscattering geometry with a confocal Raman microscope equipped with an Olympus LMPlanFL 50x objective and with a resolution of 2 cm^{-1}. The detection of Raman signal was carried out with a Peltier-cooled CCD camera. Laser power of 100 mW was used in our measurements.

UV–vis spectra were recorded using a Shimatzu 1605 UV in a quartz cuvette. The cuvette contained 0.1 mL of solution in 1 mL of PBS (pH 7.45). The spectra of individual compounds and those describing interactions between HAOA and GdAOA with the components of the model system X/XO were recorded against PBS, xanthine, or XO dissolved in PBS.

2.2. *Pharmacology*

2.2.1. Reagents. All chemicals (Sigma-Aldrich) used for the pharmacological screening were of finest grade. Bidistilled water was used to produce 50-mM Na, K Phosphate buffer (PBS, pH 7.4). Aqueous solution of MTT (3 mg/mL) was prepared to estimate the free radical accumulation in the model system Xanthine/Xanthine oxidase. The xanthine solution was 3 mM in bidistilled water. Xanthine oxidase (Sigma-Aldrich) was dissolved in 50 mM PBS to 0.2 mU/mL. HAOA and GdAOA were dissolved in PBS to molarities of 10^{-2}, 5.10^{-3}, 10^{-3}, 10^{-4}, 10^{-5}, 10^{-6}, 5.10^{-7}, 10^{-7}, and 10^{-8}. For the assessment of the Gd(III) effect on the oxidative properties, solutions of $Gd(NO_3)_3$ and $NaNO_3$ of the above-mentioned concentrations were prepared, using water-free dimethylsulfoxide (DMSO) as solvent (the gadolinium nitrate has low solubility in water).

2.2.2. Methods. In the present study, we performed comparative evaluation of the antioxidant effects of the ligand and the newly synthesized gadolinium(III) complex using several methods.

The effect of HAOA and GdAOA on free radical formation in the presence of the model system Xanthine/Xanthine oxidase (X/XO) was investigated using nitroblue tetrazolium (MTT) molecule as marker. The formation of MTT formazan was monitored by measuring the intensity of the characteristic band for the MTT formazan at 576 nm for 5 min. One mL

of the cuvette contained 0.1 mL of the nitrate (dissolved in DMSO), 0.025 mL of xanthine, 0.025 mL of XO solution, and 0.05 mL of MTT and PBS. The activity of XO was estimated by recording the spectrum of the reaction mixture in a very fast regime, each minute, for 5 min. Then the relative change of the signal for uric acid (UA) was estimated at 293 nm. Each experiment was repeated seven times; the average values and standard deviations were calculated and used for the illustrations and discussions.

The results were presented as spectrophotometric scavenging indices (SPh–SI, in %):

$$\mathrm{SPh-SI} = \frac{A^{\mathrm{sample}}}{A^{\mathrm{control}}} \times 100$$

where A^{sample} was measured in presence of GdAOA or HAOA; A^{control} was monitored in the presence of the X/XO system alone. The effect of Gd(III) on free radical formation in the model X/XO system was assessed using $NaNO_3$ as a control. The individual effects of HAOA and Gd(III) on the free radical accumulation were estimated by comparing SPh–SI for GdAOA with those of Gd(III) ion and HAOA.

The data were presented as average values and standard deviations. The statistical verifications for significance were made using the INSTAT program package. Only statistically significant results were discussed. The concentrations corresponding to the half-effect of the compounds on the accumulation of free radicals, C_{50}, were determined too and used to compare the effects of the ligands and Gd(III) on the oxidative behavior of the complex.

The antioxidant capacities of HAOA and GdAOA were investigated *in vitro* using both $DPPH^{\cdot}$ (2,2-diphenyl-1-picrylhydrazyl radical, Sigma-Aldrich) and $ABTS^{\cdot+}$ (2,2′-azinobis (3-ethylbenzothiazoline-6-sulfonic acid, Sigma-Aldrich, diammonium salt) methods. The 0.05 mM stock solution of $DPPH^{\cdot}$ was prepared using pure ethanol, immediately before the experiment, and kept in a refrigerator in a flask covered by aluminum foil. The test tubes for the DPPH experiment were covered by aluminum foil too, to prevent the effect of light on the color of the DPPH solution. $DPPH^{\cdot}$ is a stable radical, which reacts with antioxidants that can donate hydrogen. After accepting hydrogen by the antioxidant, $DPPH^{\cdot}$ which exhibits absorption at 517 nm, transforms into a product that is light yellow. The relative decrease in the purple color of the solution with time is an indication of antioxidant activity of the solution tested. Our test tubes contained 2.00 mL of DPPH stock solution, 0.02 mL of the tested solution, or 0.02 mL of PBS, or 0.02 mL of ethanol. The absorbance at 517 nm was measured after keeping the test tubes in the dark, at room temperature, for 90 min. The antioxidant activity (% scavenging) was determined by the following formula:

$$\%\,\mathrm{Scavenging} = 100 - \frac{A_b - A_c}{A_a} \times 100,$$

where A_a is the absorbance at 517 nm of the incubated test tube with DPPH stock solution (control), A_b is the absorbance of the flask containing incubated DPPH stock solution and 0.2 mL test solution (sample), and A_c is the absorbance of the DPPH containing 0.02 mL PBS (blank). Reference cuvette with pure ethanol was used during the measurements. Each absorbance A_i ($i = a, b, c$), was evaluated by five parallel measurements.

The $ABTS^{\cdot+}$ reacts with electron donors, resulting in a compound which does not absorb at 734 nm. Therefore, in the presence of antioxidants which are electron donors, the absorbance at 734 nm diminished as the antioxidant's concentration. The ABTS radical cation ($ABTS^{\bullet+}$) was prepared by mixing 7 mM ABTS with 2.45 mM potassium persulfate to final

concentration of 2.45 mM $K_2O_8S_2$ using distilled water as solvent for all solutions. The ABTS stock solution was kept in dark at room temperature for 16 h before using (in addition, the flask was covered by aluminum foil). Before the experiment, the absorbance at 734 nm of the stock solution was adjusted to 0.7000 ± 0.0004 a.u. with pure ethanol. The reference cuvette contained the same amount of ethanol as the control probe in distilled water. Five test tubes, containing 2.00 mL of ABTS stock solution and covered with aluminum foil, were prepared for each group of measurements. The absorbance at 734 nm was detected, in the cuvettes containing 2.00 mL of ABTS and 0.02 mL of PBS (blank), or 0.02 mL of test solution (sample), or 0.02 mL of ABTS stock solution (control). The % scavenging was determined using the same formula as for DPPH. The average value and standard deviation were determined for each concentration assessed and used for data presentation as dose-response curves. The concentrations exhibiting half-effect, C_{50}, were determined and used to compare the *in vitro* antioxidant properties of the compounds investigated. Solutions of ascorbate of 10^{-2}–10^{-8} M were prepared and used for building a standard curve needed to calculate the antioxidant capacity of the complexes at their C_{50} concentrations using the ABTS method.

3. Results and discussion

3.1. *Chemistry*

3.1.1. Coordination ability of 5-aminoorotic acid to Gd(III). Reaction of Gd(III) and 5-aminoorotic acid (figure 2) afforded a complex which was stable both in solid state and solution. The new Gd(III) complex was characterized by elemental analysis. The content of the metal ion was determined after mineralization. The used spectral analyses confirmed the nature of the complex.

The data of the elemental analysis of the Gd(III) complex serve as a basis for determination of its empirical formula and the results are presented below. The elemental analyses of $Gd(AOA)_3{\cdot}3H_2O$ are shown as % calculated/found: $C = 24.96/24.92$; $H = 2.49/2.35$; $N = 17.47/17.11$; $H_2O = 7.49/7.25$; Gd = 21.77/22.06, where HAOA = $C_5N_3O_4H_5$ and AOA = $C_5N_3O_4H_4^-$.

In our previous work, the geometry of 5-aminoorotic acid was computed and optimized with the Gaussian 03 program employing the B3PW91 and B3LYP methods with the 6 – 311 ++ G** and LANL2DZ basis sets [18]. In the present study, the binding mode of the HAOA ligand to Gd(III) ions is elucidated by recording IR and Raman spectra of the complex in comparison with those of free ligand. The density functional theory (DFT) calculated geometries, harmonic vibrational wavenumbers including IR and Raman scattering activities for the ligand and its complex were in good agreement with the experimental data, and a complete vibrational assignment is proposed.

3.1.2. Vibrational spectral analysis. Because no crystal structure data are available for HAOA, its structure was optimized at different levels of theory [18] and compared with literature data for compounds containing identical or similar functional groups [26–32]. Previously published X-ray diffraction data about orotic acid [26, 28] helped. The HAOA molecule has a planar structure which is very similar to the structure of orotic acid obtained

by X-ray diffraction [18, 26]. In the calculated solid-state conformation of HAOA, the existence of intramolecular hydrogen bondings is highly probable [18]. HAOA has a good ability to adopt several modes of intramolecular hydrogen bonding [27, 31], which take place between the coordinated carboxylate O1 and one of the protons of amino group, between the pyrimidine carbonyl oxygen O4 and the other proton of amino group, and between the carboxylate O3 and the imido N1–H1 (figure 2). Taking into account the average calculated hydrogen bond lengths, the latter is particularly strong. The intramolecular hydrogen bonds play an important function in the crystal packing and have influence on the respective vibrational spectra. Additionally, the geometry of La(III) complex of 5-aminoorotic acid was computed and optimized with B3PW91/LANL2DZ and B3LYP/LANL2DZ methods [18]. Through the DFT calculations with different bases, HAOA coordinated to the lanthanum ion as a dianion and the complex contained three HAOA ligands. 5-aminoorotic acid binds to La(III) through both oxygens of the carboxylic group from all three ligands; the La(III) is six coordinate in a trigonal prismatic structure [18]. Different kinds of hydrogen bonds were observed in the La(III) complex of 5-aminoorotic acid [18]: hydrogen bonding of coordinated carboxylic oxygen and the proton of nitrogen; hydrogen bonding of uncoordinated carbonylic oxygen from the pyrimidine rings and a proton of the amino group, and hydrogen bonding of the coordinated carboxylic oxygen and the other proton of the amino group. The theoretical study performed earlier has helped us to interpret the vibrational IR and Raman spectra of the newly synthesized Gd(III) complex.

The vibrational fundamentals from the IR and Raman spectra, presented in figures 3 and 4, were analyzed by comparing these modes with those from the literature [26–28, 33–42] and in combination with the results of our DFT calculations (i.e. harmonic vibrational wavenumbers and their Raman scattering activities) [18]. The selected experimental IR and Raman data of the ligand and the newly synthesized Gd(III) complex together with their tentative assignments are given in table 1. Vibrational spectra of HAOA and its Gd(III) complex are relatively

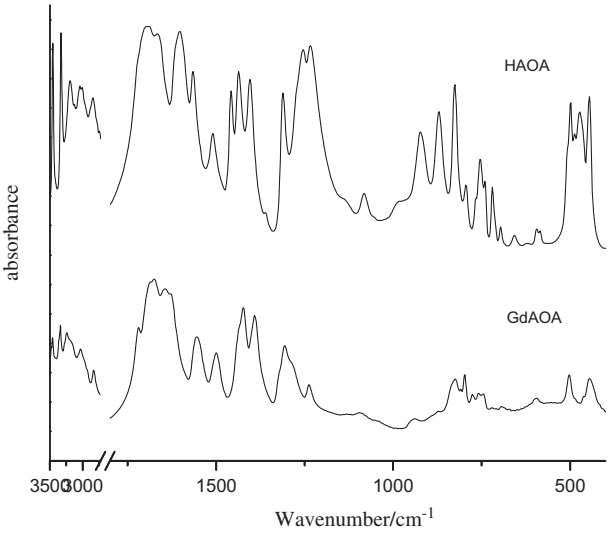

Figure 3. IR spectra of 5-aminoorotic acid (HAOA) and its Gd(III) complex.

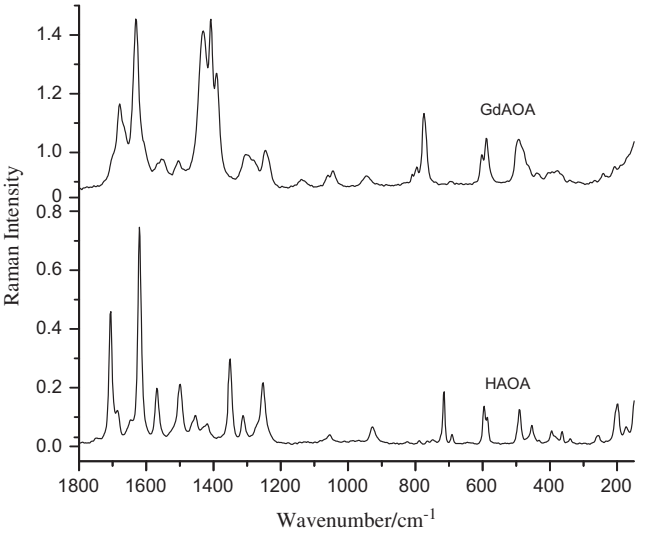

Figure 4. Raman spectra of the solid state of 5-aminoorotic acid (HAOA) and its Gd(III) complex. Excitation: 514.5 nm, 100 mW.

complex (figures 3 and 4). Several contributions of relatively high IR intensity were found, corresponding to carbonyl, carboxylic and C=C stretches, and amino-bending vibrations, which appear strongly coupled. The assignment of the bands is quite difficult because they are overlapped in the same spectral region, and the involvement of these groups in hydrogen bonds affects their wavenumbers and produces band broadening [27, 33–37].

3.1.2.1. *N–H modes.* The ν(N1–H1) and ν(N3–H3) wavenumbers in HAOA appear little affected due to the intermolecular H-bonds. In the IR spectra, the strong band at 3457 cm^{-1} (HAOA) and the band at 3443 cm^{-1} (Gd(III) complex of HAOA) were assigned to the N1–H1 stretches from the pyrimidine rings (table 1) [30, 32, 43], while the bands at 3333 cm^{-1} in the IR spectrum of HAOA and at 3335 cm^{-1} from the IR spectrum of Gd(III) complex of HAOA were attributed to the N3–H3 stretches [26, 32, 44] (figure 3, table 1). In Raman spectra, the N3–H3 stretching vibrations are present for the ligand and for the complex (table 1, figure 4). The observed experimental IR bands at 3044 and 3011 cm^{-1} could be tentatively ascribed to intermolecular H-bonds. The experimental IR bands at 2850 cm^{-1} (HAOA) and at 2839 cm^{-1} (Gd(III) complex of HAOA) correspond also to these H-bonds. In the in-plane N–H bending modes, the main contributions correspond to δ(N1–H1) and δ(N3–H3) which appear as IR bands with medium intensity at 1405 and 1436 cm^{-1} (HAOA) and at 1390 and 1424 cm^{-1} (Gd(III) complex). The experimental Raman band corresponding to δ(N1–H1) mode was not detected in the Raman spectrum of the ligand. These modes appear strongly coupled with δ(ring) modes. In general, all the vibrations in the range 1500–950 cm^{-1} have significant contributions of δ(N–H) modes. In the out-of-plane N–H bending modes, the main contribution corresponds to γ(N3–H3) mode with weak IR intensity and no Raman intensity, appearing as an IR band at 871 cm^{-1} (HAOA) and at 874 cm^{-1} (Gd(III) complex). The γ(N1–H1) mode possesses almost no IR and Raman intensity and has not been detected in the experimental spectra.

Table 1. Selected experimental IR and Raman wavenumbers (cm^{-1}) of 5-aminoorotic acid (HAOA) and its Gd(III) complex and their tentative assignment.

IR		Raman solid		
HAOA	$Gd(AOA)_3$	HAOA	$Gd(AOA)_3$	Vibrational assignment
3457 s	3443 w	3456 vw		ν(N1H1)[30, 32, 42, 43]
	3353 m		3357 w	$\nu_{as}(NH_2)$[44]
3333 s	3335 m	3323 m	3333 w	ν(N3H3)[42]
3196 m	3167 m	3166 vw		$\nu_s(NH_2)$[44]
2850 w	2839 w/m			Bonded NH···O[44]
1691 vs	1718 m	1699 m		δ(NH)[42]; ν_s(C2=O2)[28, 43], ν(Nl–C6)[42]
	1690 vs			ν_s(C4=O4)
1667 s	1674 vs	1678 sh	1681 m	ν_s(C4=O4)[50]; $\nu(COO^-)$[29, 43], ν(C5=C6), δ(N3–H3)[42]
1604 s	1644 vs	1612 vs	1629 vs	ν(C5=C6)[28, 44]; $\beta(NH_2)$, $\nu(COO^-)$[42]
1566 m	1552 m	1560 m	1545 w/m	δ_{ip}(N1H1, N5H5); ν(C5C6)[43], $\beta_s(NH_2)$[42]
1511 w	1498 m	1492 w/m	1500 w	δ(NC)[27]; ν(ring)[26, 43]; δ_{ip}(N3H3)[26]
1457 m		1447 w	1432 w	ν(ring), $\beta_s(NH_2)$, δ(Nl–H1)[26], $\nu(COO^-)$[42]
1436 m	1424 s	1421 w	1406 vs	δ(N3H3), δ(ring), δ(N1H1)[42]
1405 m	1390 s		1387 s	δ(N3H3), δ(ring), δ(N1H1)[42, 43], $\nu_s(COO^-)$[29]
1312 m	1307 m	1301 w	1302 m/s	ν(C5–N), ν(C–N), δ(OH), $\beta_s(NH_2)$[42]
1255 m/s	1284 sh			ν(C–N), δ(N1H1), $r(NH_2)$, δ(ring)[42]
1234 m/s	1239 w	1242 m	1241 m/s	ν(C–N), δ(N3H3)[26, 43], $r(NH_2)$, δ(NlH1)[42]
1140 sh	1126 vw		1130 vw	δ(OH)[42]
1083 vw		1047 vw	1043 w	ν(C6-O, C6-C7)[26, 32], $\beta_{as}(NH_2)$[42]
989 sh				ν(NCN), δ(N3H3), $r(NH_2)$, δ(NlH1)[42]
924 w	943 sh	919 w/m	946 w/m	ν(NCC), ν(ring), $r(NH_2)$, ν(COO)[42]
871 w/m	874 vw			γ(N3–H3), γ(ring)[42, 43]
795 vw	797 m/807	809 vw	780 sh	δ_{op}(O3C7O1)[27]
767 vw	776 w		776 m	γ(C4=O4), γ(C4–C=C6), γ(C6–C12)[42]
754 w	758 w	748 vw		γ(C6–C12), γ(C4=O4), γ(COOH), γ(N3–H)[42]
740 w	745 w			γ(C2=O2), γ(NC2 N), γ(N3–H)[42]
696 vw	693 vw			δ(ring), Δ_sCOO), $r(NH_2)$[42]
	601 vw			ν(Gd–O)
584 vw	594 vw	582 w	588 w/m	δ(ring), Δ_s(COO)[42]
	506 sh			ν(Gd–O)[27]
488 w	501 w	482 w/m	493 m	δ(ring), $\delta(NH_2)$, Δ_s(COO)[42]
474 w/m	461 sh			γ(OH)[42]
446 m	443 m	445 w		δ(OCNCO), δ(COO) + r(NH_2)[26, 42]

423 sh	425 sh	436 w/m	τ(C2O2, ring)[26], Δ_{as}(COO)[42]
	381 vw	373 w	δ(OCCN11), δ(COO), δ(C2=O), r(NH_2)[26, 42]; ν(Gd-O)[27]
	249 w	242 w	τ(NH_2)[26], Δ_s(COO)[42]
		207 w	ν(O–Gd–O)[27]
	196 w	183 sh	τ(ring); δ(O–Gd–O)

Notes: vw – very weak; w – weak; m – medium; ms – medium strong; s – strong; vs – very strong; sh – shoulder; ν – stretching; δ – bending; τ – torsion; s– symmetric; as– asymmetric; def. – deformation; ip – in plane; op – out of plane; ring – pyrimidine ring; sciss – scissoring; wagg – wagging.

3.1.2.2. *NH_2 group vibrations.* The NH_2 asymmetrical stretching mode that is absent in the IR and Raman spectra of the ligand can be seen in the IR and Raman spectra of the complex at 3353 cm^{-1} as a medium band (IR) and 3357 cm^{-1} as a weak band (Raman), whereas the symmetrical NH_2 stretch is present in both IR spectra by bands with medium relative intensity at 3196 and 3167 cm^{-1} and in Raman spectra of the ligand as a very weak band at 3166 cm^{-1} [44]. Moreover, the wavenumber region 2700–3000 cm^{-1} in the IR spectra of HAOA and its Gd(III) complex is typical of strongly hydrogen-bonded intermolecular complexes due to a strong anharmonic coupling (Fermi resonance) of the N–H stretching vibrations with overtones and combinations of lower frequency modes of the bonded molecules [44–46]. The β_s scissors deformation appears strongly coupled with ν(C–C=C) mode, which is in excellent agreement with the experimental IR bands detected at 1566 cm^{-1} (HAOA) and at 1552 cm^{-1} (Gd(III) complex). The rocking mode, denoted as r or β_{as}, appears strongly coupled with ν(COO) vibrations in HAOA and is assigned to the experimental IR band at 1083 cm^{-1} and to the Raman band at 1047 cm^{-1} (HAOA). In the solid state, due to NH_2 strongly H bonded with the C=O group, it is expected to increase the N–H bond lengths, and consequently, an increase in the wavenumber of the wagging mode. The value of the torsional mode $\tau(NH_2)$ in HAOA is due to an almost planar NH_2 group and a nearly pure sp^2 hybridization.

3.1.2.3. *C=O modes.* The C=O groups are very important as they take part in hydrogen bonding, especially in nucleic acid base derivatives. When the carbonyl is hydrogen bonded but not dimerized, a bond active in the IR spectra appears at 2700–3000 cm^{-1} and also another bond active in both IR and Raman spectra appears at 1730–1705 cm^{-1} [43]. In our IR spectra, these bands with medium and weak intensities for the ligand and the complex, respectively, can be observed at 2850 and 2839 cm^{-1}. One very strong band can be observed in the 1730–1690 cm^{-1} region at 1691 cm^{-1} in the IR spectrum of the ligand and one medium band at 1718 cm^{-1} in the IR spectrum of the complex, which were assigned to the symmetrical stretch of C2=O2 (figure 3). In contrast to the IR spectra, in this region of the Raman spectra, only a medium band at 1699 cm^{-1} for the free ligand was observed. The ν(C2=O2) position remains almost unaffected by changes in the molecular structure of the uracil ring. This is caused by the fact that the C2=O2 group is quite distanced from the COOH and NH_2 groups, and moreover, it is surrounded by the two N–H groups, which buffer it from influences of the remaining molecular moieties [42]. On the other hand, the C4=O4 moiety is nearer to the NH_2 group, and due to an intramolecular contact between them, the N–H and C4=O4 bonds appear slightly lengthened [42]. The dimer form is best characterized by the Raman bands at 1680–1640 cm^{-1} [38–40] and by IR bands, around 1290 cm^{-1} and between 1440 and 1395 cm^{-1} (C–O stretching mode) (figures 3 and 4; table 1) [41, 43]. The strong band at 1667 cm^{-1} from the IR spectrum of HAOA and the two very strong bands at 1690 and 1674 cm^{-1} from the IR spectrum of the complex were assigned to the symmetrical stretching modes of C4=O4 [28] and to the asymmetrical COO^- stretching modes [29, 43]. In the Raman spectra, these vibrations can be observed as a shoulder at 1678 cm^{-1} for the ligand and as a medium band at 1681 cm^{-1} for its Gd(III) complex (table 1; figures 3 and 4). The in-plane bending modes appear strongly coupled with δ(COO) modes. The out-of-plane bending modes are also strongly coupled with ring modes [42]. The γ(C4=O4) appears as a very weak experimental band at 767 cm^{-1} (IR spectrum of the ligand) and at 776 cm^{-1} (IR spectrum of Gd(III) complex). The same band seems to be absent in the Raman spectrum of the ligand and appears in the Raman spectrum of the complex (at 776 cm^{-1}). The γ(C2=O2) mode is at 740 cm^{-1} (IR spectrum of the

ligand) and at 745 cm^{-1} (IR spectrum of Gd(III) complex) with very weak IR intensity and no Raman intensity.

3.1.2.4. *C–C and C–N ring modes.* When the protons of $–NH_2$ are engaged in intramolecular hydrogen bonding, the electron lone pair of N is coupled more readily with the π-electrons of the C5=C6 bond. In IR spectra of HAOA and its Gd(III) complex, the strong and very strong bands at 1604 and 1644 cm^{-1}, respectively, were attributed to the C5=C6 stretches, NH_2 scissoring and $\nu(COO^-)$ vibration [28, 43, 44], whereas in the Raman spectra, these vibrational modes are distinguished through the very strong bands at 1612 cm^{-1} for the ligand and at 1631 cm^{-1} for its Gd(III) complex. An increase in the ν(C=C) wavenumber in the ligand appears related to an increment in the negative charge on the substituent in position 5. The medium bands from the IR spectra at 1566 cm^{-1} (ligand) and 1552 cm^{-1} (Gd(III) complex) as well as the medium peaks from the Raman spectra at 1560 cm^{-1} (ligand) and 1545 cm^{-1} (Gd(III) complex), were attributed to the C5=C6 stretching and in-plane N–H bending modes (table 1). The next pyrimidine ring vibrations, as N–C and N–H bending modes, can be observed at 1520–1490 cm^{-1} (table 1; figures 3 and 4). In IR spectra, the medium band at 1312 cm^{-1} for HAOA as well as the medium signal at 1307 cm^{-1} for the complex were attributed to the C5–N stretches (figure 3), while in the Raman spectra, these vibrations can be observed as a weak peak at 1301 cm^{-1} for the ligand and as a medium/strong signal at 1302 cm^{-1} for the complex, shifted to lower wavenumbers (table 1; figure 4).

The IR band at 1255 cm^{-1} was assigned as ν(C–N). This mode was detected only in IR spectra for the free ligand and blue shifted 30 cm^{-1} for the complex (1284 cm^{-1}). The experimental IR bands at 1234, 989, and 924 cm^{-1} in the spectrum of the ligand are also C–N stretches. The last two bands were detected with weak intensity. These modes appear in both IR and Raman spectra of the free ligand and the complex. In the IR spectra, they can be seen at 1234 and 1239 cm^{-1}, while in the Raman spectra, they are situated at 1242 and 1241 cm^{-1}, respectively (table 1). The very weak signal at 989 cm^{-1} in the IR spectrum of the ligand (absent in the IR spectrum of the complex), assigned to the trigonal pyrimidine ring breathing mode [26, 43], cannot be observed in the corresponding Raman spectra.

3.1.1.5. *COOH group vibrations.* The ν(O–H) and γ(O–H) modes are characterized as almost pure modes. The IR shoulder at 1140 cm^{-1} in the IR spectrum of the HAOA is assigned to the in-plane δ(OH) bend. This mode appears as a weak peak at 1126 cm^{-1} in the IR spectrum of Gd(III) complex, whereas in the Raman spectra can be seen just for the complex as a very weak peak at 1130 cm^{-1}. The strong IR band at 1667 cm^{-1} is tentatively assigned to the ν(C=O) of the carboxylic group of the ligand. Strong H-bonds are expected in the solid state through this group. The experimental Raman band in the spectrum of the free ligand at 1341 cm^{-1} was assigned as ν(C–O) stretch as a medium signal. The Raman bands at 425 and 249 cm^{-1} (HAOA) and at 436 and 242 cm^{-1} (Gd(III) complex of HAOA) were assigned as $\Delta_{as}(COO)$ and $\Delta_s(COO)$ modes, respectively. The symmetrical COO^- stretch was observed in IR spectra as medium and strong bands at 1405 and 1390 cm^{-1} for the ligand and its Gd(III) complex, respectively, while in the Raman spectra, this vibration appears as a strong peak at 1387 cm^{-1} only for the complex (figures 3 and 4).

In general, between the IR and Raman spectra of the ligand in comparison to the same spectra of the metal complex, we can assert wavenumbers shifting, increases and/or decreases in relative intensities, and appearances and/or disappearings of bands. These

changes can be caused by decrease in the force constants of the bonds and polarization of the C–C and C–H bonds in the pyrimidine rings [30]. The formation of complexes with lanthanides perturbs not only the aromatic systems of the rings, but also the quasi-aromatic systems [47–53]. The metal affects the Gd–O bonds and this effect is transferred to the C–O bonds. After that, the force constant of OCC_{ring} bond is changed, which reflects in the displacement of electronic charge around bonds between heterocyclic rings, and heterocyclic rings and protons [53]. The pyrimidine ring bending vibration and the skeletal deformation bands of the free ligand, mainly at 900–300 cm^{-1} wavenumber region, show considerable changes on complex formation (figures 3 and 4; table 1). These changes may be attributed to distorsion of the pyrimidine rings upon complexation.

Spectra below 600 cm^{-1} are particularly interesting since they provide information about metal–ligand vibrations. The new band at 601 cm^{-1} and the new shoulder at 506 cm^{-1} present only in the IR spectrum of the complex (not observed in its Raman spectrum) can be due to the Gd–O interactions [27, 28, 37]. In the low wavenumber region of the Raman spectrum of the complex (figure 4), the band that can be due to the Gd–O vibrations [48–52] is the band at 373 cm^{-1}. Besides the appearance of a new shoulder at 423 cm^{-1} in the IR spectrum of the ligand confirms the presence of the Gd–O interaction. The metal affects the carboxylate anion as well as the ring structure. The ionic potential of the metal is the most important parameter responsible for the influence of the metal on the rest of the molecule [53–55]. The carboxylic acids interact with the metals as symmetric [56, 57], bidentate carboxylate anions and both oxygens of the carboxylate are symmetrically bonded to the metal [58]. We can observe in the Raman spectrum of the Gd(III) complex a weak peak at 207 cm^{-1}, which can be due to the O1–Gd–O3 vibration modes (table 1) [52, 59–61].

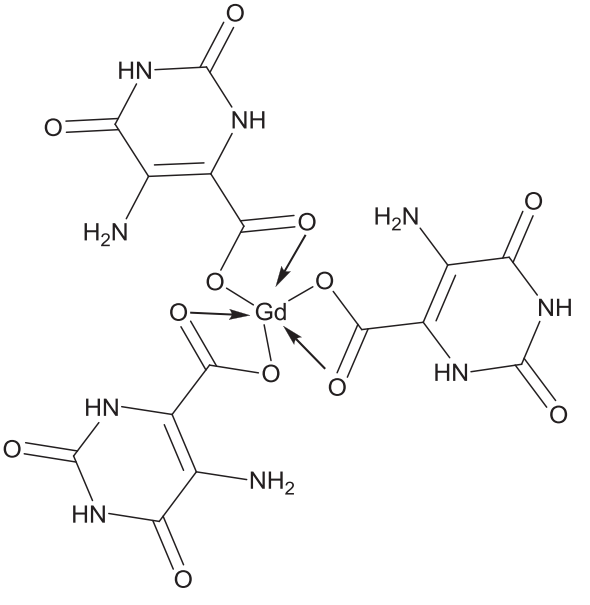

Figure 5. Suggested metal–ligand coordination in the investigated Gd(III) complex.

Thus, on the basis of the experimental and theoretical results, we are able to suggest that in the Gd(III) complex studied, the metal ion coordinated to the carboxylic oxygens, as shown in figure 5.

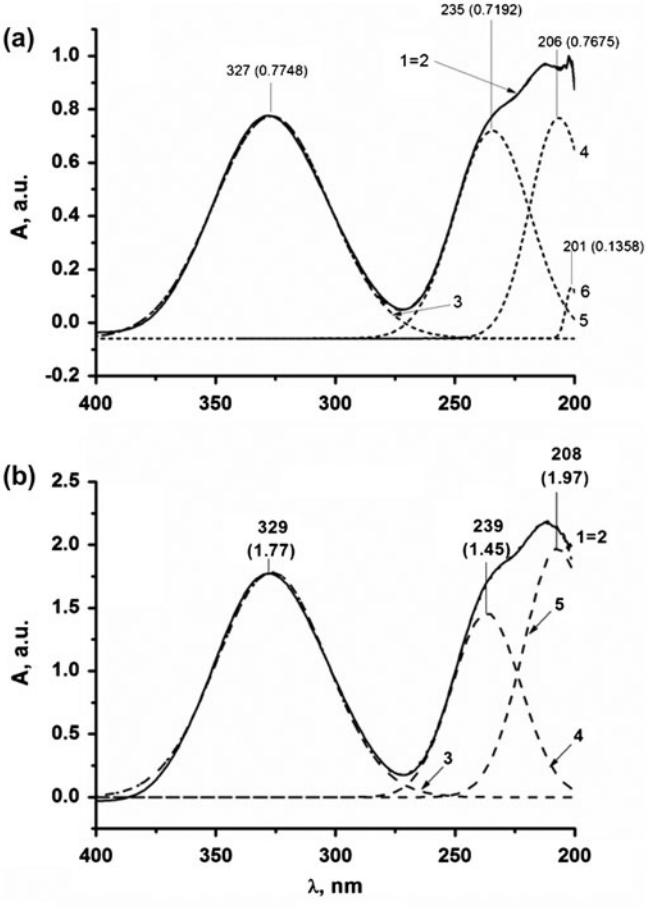

Figure 6. Deconvolution of the spectra of HAOA and GdAOA: 1 – real spectrum, 2 – mathematical result based on the deconvolution, 3, 4, 5, and 6 – components of the band, found after its deconvolution.

Table 2. Assignments of the characteristic bands corresponding to the components of the UV spectra of HAOA and GdAOA, according to the literature data.

Characteristic UV band (nm)	Assignment
325	Characteristic band of the ring in the HAOA molecule
235	$\pi \rightarrow \pi^*$ transition of the triple conjugated double-bond system in the AOA molecule
206	A possible E2 – type ($\pi \rightarrow \pi^*$) of characteristic band of the C=O and C=C groups in the molecule
201	$\pi \rightarrow \pi^*$ transition of C=O groups in C(O)OH

3.1.3. UV spectra of HAOA and GdAOA. The UV spectra of 10^{-4} M HAOA and GdAOA are presented in figure 6. Their spectra consist of four components with λ at about 327, 235, 206, and 201 nm. In agreement with the literature data [62, 63], these bands were assigned as shown in table 2.

In the spectrum of HAOA [figure 6(a)], all components listed in table 2 were present, which was in agreement with the structure of this compound (figure 2). In the spectrum of GdAOA, the characteristic band for the COOH group at 201 nm was missing, and this was in agreement with the structure of the GdAOA molecule (figure 5). The GdAOA complex (figure 5) contained three AOA ligands, and this would lead to a ratio between the intensities of the AOA characteristic bands at 3. The average ratio between absorptions was 2.3 ± 0.3. This, along with the very mild red shift of all bands in GdAOA compared to the HAOA spectrum, indicated that the main effect of Gd(III) on the ligand was a decrease in the dipole moment.

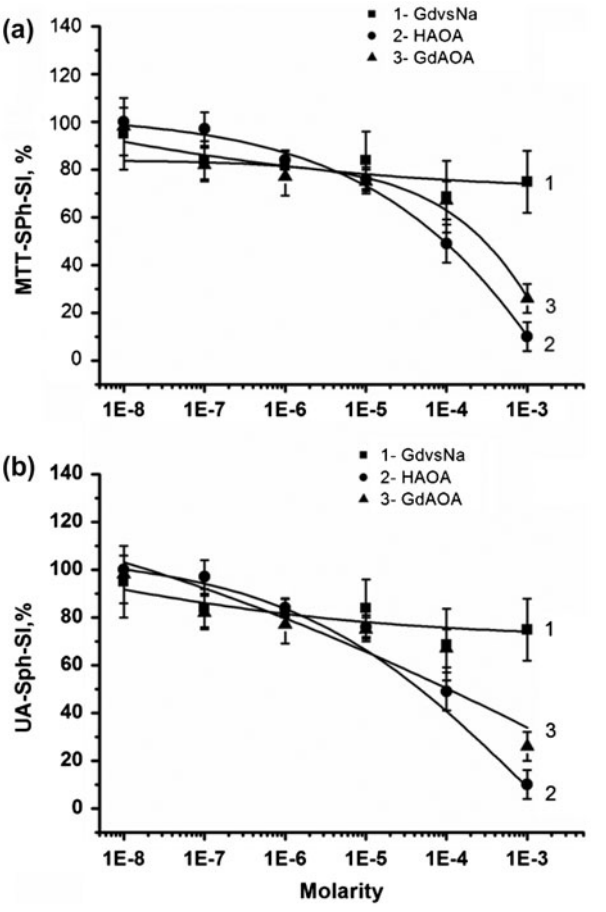

Figure 7. Accumulation of free radicals in the model system X/XO (presented as MTT Formazan's SPh-SI, %) – (a), and of UA (presented as UA Formazan's SPh–SI, %) – (b): curve 1 – in the presence of $Gd(NO_3)_3$ (dissolved in DMSO with control sample $NaNO_3$ in DMSO); curves 2 and 3 illustrate the effects of HAOA and GdAOA, respectively, in PBS, using X/XO alone as a control sample.

3.2. *Pharmacology*

GdAOA exhibited antioxidant properties (figure 7) in the presence of the X/XO model system. Curve 1 in figure 7(a) and (b) shows that, compared with Na(I), Gd(III) exhibited mild antioxidant effect. Looking at the accumulation of free radicals [figure 7(a)] and of UA [figure 7(b)], a substantial antioxidant effect of GdAOA was observed. Although below concentrations of 10^{-5} M, both compounds showed almost the same antioxidant activity, above this concentration HAOA was a better antioxidant (curves 2 and 3). The comparisons for the overall antioxidant activity were made using the concentrations at which 50% of the antioxidant effect was achieved, C_{50}. For the free radical accumulation [figure 7(a)], HAOA and GdAOA exhibited C_{50} of $(8 \pm 2)\cdot10^{-5}$ M and $(4 \pm 1)\cdot10^{-4}$ M, respectively. The C_{50} values for the accumulation of UA were $(4 \pm 1)\cdot10^{-5}$ M and $(2.2 \pm 0.7)\cdot10^{-4}$ M for HAOA and GdAOA, respectively.

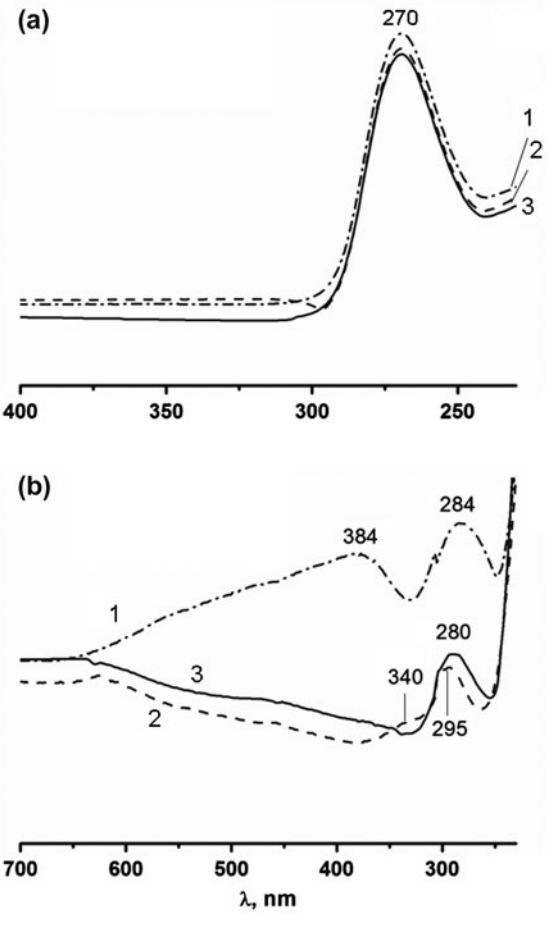

Figure 8. UV spectra of Xanthine (a) and Xanthine oxidase (b) in PBS, alone, or in presence of 10^{-6} M solutions of GdAOA and HAOA: spectrum 1 was recorded in the presence of GdAOA, spectrum 2 – in the presence of HAOA, spectrum 3 was either of Xanthine (a) or XO (b) alone. Xanthine and Xanthine oxidase were of concentrations as in the pharmacological experiments.

A compound may exhibit antioxidant activity by scavenging the free radicals produced in the medium, or by inhibiting the enzyme responsible for free radical production. In the X/XO model system, the formation of free radicals is a result of the activity of the xanthine oxidase. Another opportunity is an interaction between the compound and xanthine. In the presence of the X/XO model system, xanthine transforms over the catalyst, XO, to UA and superoxide radical $O_2^{\cdot-}$. Interaction of GdAOA or HAOA with xanthine may alter the X/XO interactions. To elucidate the action of the compounds investigated, we assessed their abilities to interact with xanthine and xanthine oxidase. UV spectra were recorded for X and XO alone, and in presence of HAOA or GdAOA. Both the latter spectra were corrected for the compound investigated. This permitted seeing only the UV spectrum of xanthine or xanthine oxidase. Interactions within the components of the model system X/XO and the compounds investigated were explored by comparing UV spectra of the pure components with those in the presence of HAOA or GdAOA (figure 8). The effects of HAOA and GdAOA on the UV spectrum of xanthine [figure 8(a)] were less prominent than those on the XO spectrum [figure 8(b)]. In figure 8(a), the UV spectrum of (GdAOA+X) is recorded against GdAOA (spectrum 1) and that of (HAOA+X) is corrected for HAOA (spectrum 2). In presence of GdAOA [figure 8(a), spectrum 1] and HAOA [figure 8(a), spectrum 2], the intensity of the characteristic band at 270 nm slightly increased, but did not shift by position compared with the spectrum of xanthine [figure 8(a), spectrum 3]. This might be related with a slightly increased dipole moment of the xanthine molecule in the presence of the compounds investigated. The relative change was the modest. In figure 8(b), a difference is observed in the effects of HAOA [figure 8(b), spectrum 2] and GdAOA [figure 8(b), spectrum 1] on the original spectrum of XO [figure 8(b), spectrum 3]. In agreement with previous report [64], the band at 280 nm in the UV spectrum of XO was attributed to the aromatic amino chains (affected by the solvent), and the shoulder at about 340 nm – to a molybdenum co-factor. Compared with the spectrum of XO [figure 8(b), spectrum 3], a substantial increase in the intensities of all characteristic bands for XO were observed in the presence of GdAOA [figure 8(b), spectrum 1]. This might be related with increased dipole moment and/or diminished influence of the solvent on the XO molecule. In presence of GdAOA [figure 8(b), spectrum 1], the characteristic band for the molybdenum co-factor (340 nm) shifted about 40 nm to higher wavenumbers and increased in intensity, compared with the spectrum of XO in presence of HAOA [figure 8(b), spectrum 2], and that of XO alone [figure 8(b), spectrum 3]. This indicated an interaction of XO with GdAOA, which might alter the enzymatic activity of the former. The same type of interaction, but to a much lesser extent, was seen in the spectrum of XO in the presence of HAOA [figure 8(b), spectrum 2], when compared with the spectrum of the XO alone [figure 8b, spectrum 3]. Thus, there is more substantial interaction within GdAOA and XO than for HAOA and XO. Both HAOA and GdAOA showed antioxidant properties with GdAOA being the weaker antioxidant.

Our investigations showed a mild antioxidant effect of Gd(III) compared with Na(I) under the same conditions [figure 7(a) and (b), curve 1], which might be related with the stable $4f^7$ configuration of Gd(III) [65]. The overall oxidative behavior of GdAOA was antioxidant [figure 7(a) and (b), curve 3], but slightly lower than that of HAOA [figure 7(a) and (b), curve 2]. Figure 8 indicated that Gd(III) increased the interactions of the AOA ligands with XO, compared with HAOA. The effects of GdAOA and HAOA on the UV spectrum of xanthine were almost negligible [figure 8(a)] compared to those on the XO spectrum [figure 8(b)]. The interaction between GdAOA and XO might lead to an altered

XO activity in the presence of GdAOA at high concentrations [figure 7(b), curve 3] compared with the activity of the enzyme in the presence of HAOA [figure 7(b), curve 2].

Gd(III) interacted with HAOA forming a stable complex, and this resulted in a slightly lower antioxidant activity of the ligand. Both HAOA and GdAOA did not show antioxidant activity against the stable $DPPH^{\cdot}$ radical. This indicated that the antioxidant effects observed might be related with electron donor properties of the compounds investigated toward free radicals. The ABTS test proved that HAOA and GdAOA are scavengers of $ABTS^{\cdot+}$ with C_{50} of 1.18×10^{-6} M and 4.72×10^{-6} M, respectively, with ascorbate equivalents of 2.12×10^{-4} M for HAOA and 1.68×10^{-4} M for GdAOA. The ratios between C_{50} of both compounds indicated that Gd(III) slightly decreased the electron donors' antioxidant activity of the AOA ligands in the GdAOA molecule.

4. Conclusion

The complex of Gd(III) with 5-aminoorotic acid has been synthesized and characterized by elemental and vibrational spectral analyses. IR and Raman spectra of 5-aminoorotic acid and its Gd(III) complex were recorded and the marker bands of characteristic functional groups identified, in order to use them as a data bank for further application in trace analysis of rare-earth complexes.

The vibrational analysis performed for 5-aminoorotic acid and its Gd(III) complex helped to explain the vibrational behavior of the ligand vibrational modes, sensitive to interaction with Gd(III). The vibrational studies and the previous density functional calculations revealed that the mode of binding was bidentate through carboxylic oxygens. Theoretical and spectral studies gave evidence for the coordination mode of the ligand to Gd(III) and were in agreement with the other literature studies and theory predictions.

In presence of the X/XO model system, both HAOA and GdAOA showed antioxidant properties, acting as radical scavengers via electron donation. The slightly weaker antioxidant activity of GdAOA compared to HAOA might be related with the effect of Gd(III) on the AOA ligands, leading to a decrease in their electron donor properties. The interaction within GdAOA and XO might increase the activity of the enzyme in the presence of high concentrations of the complex.

Acknowledgments

The authors gratefully acknowledge the financial support from the Medical University-Sofia Grant Commission (through Project No. 32/2014).

Disclosure statement

No potential conflict of interest was reported by the authors.

References

[1] P.L. Panzeter, D.P. Ringer. *Biochem. J.*, **293**, 775 (1993).
[2] P.J. Banditt. *J. Chromatogr. B*, **660**, 176 (1994).

[3] M.T. MacCann, M.M. Thompson, I.C. Gueron, M. Tuchman. *Clin. Chem.*, **41**, 739 (1995).
[4] O. Kumberger, J. Riede, H. Schmidbaur. *Chem. Ber.*, **124**, 2739 (1991).
[5] P. Ruasmadiedo, J.C. Badagancedo, E. Fernandez Garcia, D.G. Dellano, C.G. de los Reyes Gavilan. J. Food Prot., **59**, 502 (1996).
[6] I. Kostova, N. Peica, W. Kiefer. *Vib. Spectro.*, **44**, 209 (2007).
[7] I. Kostova, S. Balkansky, J. Mojzis. *Int. J. Curr. Chem.*, **1**, 271 (2010).
[8] W.B. Person, K. Szczepaniak, In *Vibrational Spectra and Structure*, J.R. Durig (Ed.), pp. 239–325, Elsevier, Amsterdam (1993).
[9] H. Rostkowska, K. Szczepaniak, M.J. Nowak, J. Leszczynski, K. KuBulat, W.B. Person. *J. Am. Chem. Soc.*, **112**, 2147 (1990).
[10] I.R. Gould, I.H. Hillier. *J. Chem. Soc., Perkin Trans.*, **2**, 329 (1990).
[11] G.J. Thomas Jr., M. Tsuboi, In *Advances in Biophysical Chemistry*, C.A. Bush (Ed.), pp. 1–70, JAI Press, Greenwich, CT (1993).
[12] P. Lagant, G. Vergoten, R. Efremov, W.L. Peticolas. *Spectrochim. Acta, Part A*, **50**, 961 (1994).
[13] T. Rush, W.L. Peticolas. *J. Phys. Chem.*, **99**, 14647 (1995).
[14] A. Aamouche, G. Berthier, C. Coulombeau, J.P. Flament, M. Ghomi, C. Henriet, H. Jobic, P.Y. Turpin. *Chem. Phys.*, **204**, 353 (1996).
[15] A. Aamouche, M. Ghomi, C. Coulombeau, L. Grajcar, M.H. Baron, H. Jobic, G. Berthier. *J. Phys. Chem. A*, **101**, 1808 (1997).
[16] F. Nepveu, N. Gaultier, N. Korber, J. Jaud, P. Castan. *J. Chem. Soc., Dalton Trans.*, **24**, 4005 (1995).
[17] K. Helios, M. Duczmal, A. Pietraszko, D. Michalska. *Polyhedron*, **49**, 259 (2013).
[18] I. Kostova, N. Peica, W. Kiefer. *Chem. Phys.*, **327**, 494 (2006).
[19] I. Kostova, N. Peica, W. Kiefer. *J. Raman Spectrosc.*, **38**, 205 (2007).
[20] I. Kostova, M. Traykova, V.K. Rastogi. *Med. Chem.*, **4**, 371 (2008).
[21] I. Kostova, T. Stefanova. *J. Rare Earths*, **28**, 40 (2010).
[22] I. Kostova, T. Stefanova. *J. Trace Elem. Med. Biol.*, **24**, 7 (2010).
[23] I. Kostova, M. Traykova. *Med. Chem.*, **2**, 463 (2006).
[24] I. Kostova, G. Momekov. *J. Coord. Chem.*, **61**, 3776 (2008).
[25] I. Kostova, T. Stefanova. *J. Coord. Chem.*, **62**, 3187 (2009).
[26] A. Hernanz, F. Billes, I. Bratu, R. Navarro. *Biopolymers (Bioospectroscopy)*, **57**, 187 (2000).
[27] R. Wysokiński, B. Morzyk-Ociepa, T. Głowiak, D. Michalska. *J. Mol. Struct. (Theochem)*, **606**, 241 (2002).
[28] E.J. Baran, R.C. Mercader, F. Hueso-Ureña, M.N. Moreno-Carretero, M. Quiros-Olozabal, J.M. Salas-Peregrin. *Polyhedron*, **15**, 1717 (1996).
[29] D.J. Darensbourg, J.D. Draper, D.L. Larkins, B.J. Frost, J.H. Reibenspies. *Inorg. Chem.*, **37**, 2538 (1998).
[30] W. Lewandowski, M. Kalinowska, H. Lewandowska. *J. Inorg. Biochem.*, **99**, 1407 (2005).
[31] N. Lalioti, C.P. Raptopoulou, A. Terzis, A. Panagiotopoulos, S.P. Perlepes, E. Manessi-Zoupa. *J. Chem. Soc., Dalton Trans.*, **8**, 1327 (1998).
[32] K.H. Horn, N. Böres, N. Lehnert, K. Mersmann, C. Näther, G. Peters, F. Tuczek. *Inorg. Chem.*, **44**, 3016 (2005).
[33] R.D. Batt, J.K. Martin, J. Mc, T. Ploeser, J. Murray. *J. Am. Chem. Soc.*, **76**, 3665 (1955).
[34] H. Icbudak, H. Olmez, O.Z. Yesilel, F. Arslan, P. Naumov, G. Jovanovski, A.R. Ibrahim, A. Usman, H.K. Fun, S. Chantrapromma, S.W. Ng. *J. Mol. Struct.*, **657**, 255 (2003).
[35] G.S. Papaefstathiou, S. Manessi, C.P. Raptopoulou, E.J. Behrman, T.F. Zafiropoulos. *Inorg. Chem. Commun.*, **7**, 69 (2004).
[36] J.R. Lacher, J.L. Bitner, D.J. Emery, M.E. Seffl, J.D. Park. *J. Phys. Chem.*, **59**, 610 (1955).
[37] S. Lencioni, A. Pellerito, T. Fiore, A.M. Giuliani, L. Pellerito, M.T. Cambria, C. Mansueto. *Appl. Organomet. Chem.*, **13**, 145 (1999).
[38] K. Exner, G. Fischer, N. Bahr, E. Beckmann, M. Lugan, F. Yang, G. Rihs, M. Keller, D. Hunkler, L. Knothe, H. Prinzbach. *Eur. J. Org. Chem.*, **5**, 763 (2000).
[39] J. Castaneda, G.S. Denisov, S.Y. Kucherov, V.M. Schreiber, A.V. Shurukhina. *J. Mol. Struct.*, **660**, 25 (2003).
[40] F. González-Sánchez. *Spectrochim. Acta*, **12**, 17 (1958).
[41] D. Hadzi, N. Sheppard. *Proc. R. Soc. Ser. A*, **216**, 247 (1953).
[42] S. Ortiz, M. Alcolea Palafox, V.K. Rastogi, R. Tomer. Spectrochim. Acta, Part A, **97**, 948 (2012).
[43] D. Lin-Vien, N.B. Colthup, W.G. Fateley, J.G. Grasselli. In *The Handbook of Infrared and Raman Characteristic Frequencies of Organic Molecules*, H.B. Jovanovich (Ed.), p. 140, Academic Press Inc., San Diego, CA (1991).
[44] F.R. Dolish, W.G. Fateley, F.F. Bentley, *Characteristic Raman Frequencies of Organic Compounds*, p. 128, John Wiley & Sons Inc., New York (1974).
[45] J.M. Orza, M.V. García, I. Alkorta, J. Elguero. *Spectrochim. Acta, Part A*, **56**, 1469 (2000).
[46] A. Szabó, V.I. Češljević, A. Kovács. *Chem. Phys.*, **270**, 67 (2001).
[47] W. Lewandowski, H. Barańska. *Vib. Spectrosc.*, **2**, 211 (1991).
[48] C. Sourisseau, M. Fouassier, R. Mauricot, F. Boucher, M. Evain. *J. Raman Spectrosc.*, **28**, 973 (1997).
[49] Y. Lu, G. Deng, F. Miao, Z. Li. *Carbohydr. Res.*, **338**, 2913 (2003).

[50] J.R. Sohn, E.W. Chun, Y.I. Pae. *Bull. Korean Chem. Soc.*, **24**, 1785 (2003).
[51] A. Jayaraman, S.K. Sharma, S.Y. Wang, S.R. Shieh, L.C. Ming, S.W. Cheong. *J. Raman Spectrosc.*, **27**, 485 (1996).
[52] A. Fielicke, G. Meijer, G. von Helden. *Eur. Phys. J. D*, **24**, 69 (2003).
[53] W. Lewandowski, B. Dasiewicz, P. Koczoń, J. Skierski, K. Dobrosz-Teperek, R. Świsłocka, L. Fuks, W. Priebe, A.P. Mazurek. *J. Mol. Struct.*, **604**, 189 (2002).
[54] P. Koczón, W. Lewandowski, A.P. Mazurek. *Vib. Spectrosc.*, **20**, 143 (1999).
[55] M. Kakiuchi, T. Abe, H. Nakayama. *Geochem. J.*, **35**, 285 (2001).
[56] K. Wang, Y.S. Li. *Vib. Spectrosc.*, **14**, 183 (1997).
[57] F.J. Boerio, P.P. Hong, P.J. Clark, Y. Okamoto. *Langmuir*, **6**, 721 (1990).
[58] Y.J. Kwon, D.H. Son, S.J. Ahn, M.S. Kim, K. Kim. *J. Phys. Chem.*, **98**, 8481 (1994).
[59] E. Gałdecka, Z. Gałdecki, E. Huskowska, V. Amirkhanov, J. Legendziewicz. *J. Alloys Compd.*, **257**, 182 (1997).
[60] A. de Andrés, S. Taboada, J.L. Martínez. *Phys. Rev. B*, **47**, 14898 (1993).
[61] B.O. Cho, S.X. Lao, J.P. Chang. *J. Appl. Phys.*, **93**, 9345 (2003).
[62] F.-X. Shmidt. *Encyclopedia of Life Science*, MacMillan Publishers Ltd., Nature Publishing Group, UK (2001).
[63] NPL Kale&Laby. *Table of Physical and Chemical Constants*, Chapter 3: Chemistry, Section 3.8. Molecular Spectroscopy; Subsection 3.8.7. UV- Spectroscopy. Seen in 2015, Available online at: http://www.kayelaby.npl.co.uk./chemistry/3-8/3-8-7.html
[64] M. Harizadeh, J. Keyhani, C. Khodadadi. *Acta Biochim. Biophys. Chin.*, **41**, 603 (2009).
[65] R.D. Shannon. *Acta Cryst. A*, **32**, 751 (2001). Copyright © International Union of Crystallography. Reproduced with permission.